Open access • Journal Article • DOI:10.1063/1.353338

Preparation and properties of electrodeposited indium tin oxide/SnO2/CdTe and indium tin oxide/SnO2/CdS/CdTe solar cells — Source link

S. K. Das, G. C. Morris

Published on: 15 Jan 1993 - Journal of Applied Physics (American Institute of Physics)

Topics: Indium tin oxide, Solar cell and Cadmium telluride photovoltaics

Preparation and properties of electrodeposited indium tin oxide/SnO2/CdTe and indium tin oxide/SnO2/CdS/CdTe solar cells

S. K. Das and G. C. Morris

Citation: Journal of Applied Physics **73**, 782 (1993); doi: 10.1063/1.353338
View online: http://dx.doi.org/10.1063/1.353338
View Table of Contents: http://scitation.aip.org/content/aip/journal/jap/73/2?ver=pdfcov
Published by the AIP Publishing

Preparation and properties of electrodeposited indium tin oxide/SnO_2/CdTe and indium tin oxide/SnO_2/CdS/CdTe solar cells

S. K. Das[a] and G. C. Morris
Department of Chemistry, University of Queensland, Brisbane Qld 4072, Australia

(Received 4 June 1992; accepted for publication 5 October 1992)

Cadmium telluride-based solar cells have been prepared as indium tin oxide (ITO)/SnO_2/CdTe and indium tin oxide/SnO_2/CdS/CdTe structures where CdS and CdTe were prepared by an electrodeposition technique. Both open circuit voltage and short circuit current of ITO/SnO_2/CdTe cells were higher than that of ITO/SnO_2/CdS/CdTe cells. The spectral response measurement showed that the current collection was higher in the ITO/SnO_2/CdTe cell relative to the ITO/SnO_2/CdS/CdTe cell. Current-voltage temperature measurements indicated that the junction transport could be controlled by recombination or thermally assisted tunneling in the ITO/SnO_2/CdTe cell, whereas tunneling could be the dominant junction transport mechanism in the ITO/SnO_2/CdS/CdTe cell. Activation energies of ITO/SnO_2/CdTe and ITO/SnO_2/CdS/CdTe cells were 0.60 and 0.76 eV, respectively. The values of the built-in potential, V_{bi} calculated from the measurement of open circuit voltage with temperature were 1.41 and 1.5 eV for ITO/SnO_2/CdTe and ITO/SnO_2/CdS/CdTe cells, respectively, whereas from Mott–Schottky plots they were 1.1 and 0.95 eV, respectively.

I. INTRODUCTION

Cadmium telluride-based thin-film solar cells are one of the promising photovoltaic devices for low-cost large area terrestrial application. Solar cell grade cadmium telluride has been prepared by different techniques such as close-spaced vapor transport,[1–4] screen printing,[5,6] electrodeposition,[7–13] vacuum evaporation,[14] etc. Efficient CdTe-based polycrystalline solar cells have been fabricated as CdS/CdTe,[1–14] indium tin oxide (ITO)/CdTe,[15–18] TO/CdTe,[19] ZnO/CdTe,[20–22] etc. Among the different techniques of producing cadmium telluride material, electrodeposition is one of the most suitable low-cost methods that can produce over 10% efficient CdS/CdTe[7–10] solar cells. A few groups worked on ITO/CdTe solar cells in which the CdTe was single crystal.[15–18] Panicker, Knaster, and Kroger[23] first demonstrated the cathodic electrodeposition of CdTe film from aqueous solution. In this article we describe the preparation and characterization of electrodeposited ITO/SnO_2/CdTe and ITO/SnO_2/CdS/CdTe solar cells.

II. EXPERIMENT

A. Cleaning of the substrates

The substrate material sodalime glass ITO/SnO_2 (10 $\Omega/\square$, purchased from Hoya Corporation, Japan) was cleaned by acetone, methanol, and isopropanol successively in an ultrasonic bath for 15 min in each solution followed by isopropanol vapor degreasing for 3 h.

B. Cadmium sulfide electrodeposition

A CdS deposition solution was made up as 0.2M Cd^{2+} with $CdCl_2$ (analytical reagent grade) and Milli-Q water (18 MΩ cm) from a purification system of Millipore Corporation, U.S.A. The solution was taken in a 1.5 ℓ Pyrex glass bath and maintained at 90 °C and stirred. The solution was electropurified for 12 h at +5 mV more positive potential than the measured cadmium potential. Sodium thiosulphate was added to make the solution 0.01 M $S_2O_3^-$ and the *p*H was adjusted to 2.5.

The cleaned glass/ITO/SnO_2 substrate was preheated in 90 °C Milli-Q water for 15 min and then transferred to a CdS bath solution for electrodeposition. The electrodeposition was carried out at 40 mV more positive potential than measured cadmium potential, generally +620 mV with respect to saturated calomel electrode. The counter electrode was a spectroscopic grade carbon rod placed inside a fritted glass tube to avoid broken carbon particles inside the solution. In about 2 h, about a 100-nm-thick yellow CdS layer was deposited.

C. Cadmium telluride electrodeposition

A 2.5 M Cd^{2+} bath solution was made by using $3CdSO_4 \cdot 8H_2O$ (analytical reagent grade), $CdCl_2 \cdot H_2O$ (analytical reagent grade) and Milli-Q water maintained at 90 °C and stirred. The bath solution was electropurified for 12 h at 10 mV more positive potential than measured cadmium potential. The *p*H was adjusted to 2.0 by adding H_2SO_4 (Aristar grade). The inclusion of Te ions into the solution was performed by pushing Te ions from a spectroscopic grade Te rod. The concentration of Te ions in the bath solution was measured by a computer controlled Atomic Absorption Spectrometer (Varian Spectra A300). The concentration of $HTeO_2^+$ was maintained at 120 ppm by using a split anode (Te and C) system where Te acted as both calomel electrode and the source of $HTeO_2^+$ in the solution. The CdTe depositions were carried out on glass/ITO/SnO_2 or glass/ITO/SnO_2/CdS substrates at 20 mV more positive potential than measured cadmium potential. The thickness of the CdTe layer was about 2 μm.

[a]Author to whom all correspondence should be addressed.

 0021-8979/93/020782-05$06.00

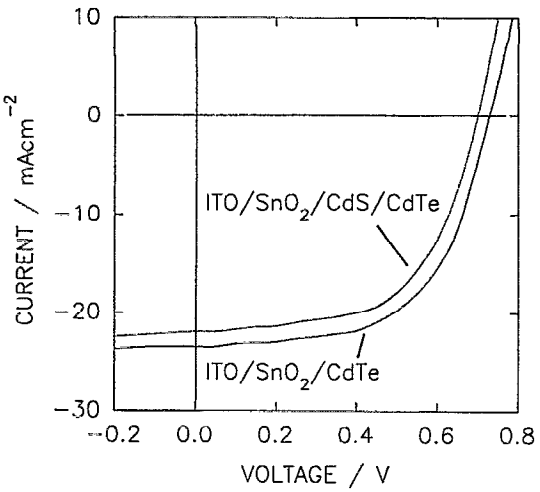

FIG. 1. Current density vs voltage (J-V) characteristics under 1000 W m^{-2} solar simulation for ITO/SnO_2/CdTe (cell A: efficiency 9.8%) and ITO/SnO_2/CdS/CdTe (cell B: efficiency 8.8%).

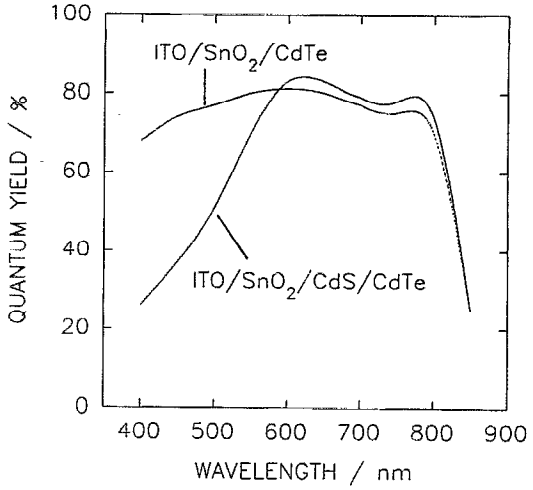

FIG. 2. Spectral response of cells A and B of Fig. 1.

D. Cells completion

After deposition of CdTe on glass/ITO/SnO_2 or glass/ITO/SnO_2/CdS substrates, the samples were kept in vacuum (10^{-4} Torr) for 12 h. Production of CdS/CdTe heterojunction required the type conversion of as-deposited n-CdTe to p-CdTe by heat treatment in air as disclosed in US patent No. 4 388 483.[24] The dry samples were annealed at 400 °C in air for 15 min for the formation of a n-CdTe/p-CdTe heterojunction. After being cooled down to room temperature, the CdTe surface was etched by using 1:1 potassium dichromate/sulphuric acid solution for 2 s and washed thoroughly with Milli-Q water. The sample was dried by nitrogen gas flow and then kept in hydrazine hydrate solution for 15 min for the reduction of the oxide layer on the CdTe surface. After hydrazine hydrate treatment, the samples were washed in Milli-Q water and dried by nitrogen gas and then immediately transferred to a vacuum chamber for copper and gold deposition for electrical contact to CdTe. At 10^{-6} Torr, 2 mm-diam cells were fabricated after deposition of 2 nm copper and 100 nm gold. The exact areas of the cells were measured under a microscope. Silver paste was added to the gold for mechanical strength.

III. PROPERTIES OF THE CELLS

Current-voltage measurements were carried out by using a computer controlled system with a 300 W Oriel simulator set to produce 1000 W m^{-2} AM1 radiation using a cell calibrated at the U.S. Solar Energy Research Institute.

Figure 1 shows the J-V plot under illumination for the ITO/SnO_2/CdTe (cell A) and ITO/SnO_2/CdS/CdTe (cell B) cells. The solar cell parameters of cell A were as $V_{oc} \approx 720$ mV, $J_{sc} \approx 23.5$ mA cm^{-2}, fill factor (FF) ≈ 0.58, and efficiency $\approx 9.8\%$, whereas for cell B were as $V_{oc} \approx 700$ mV, $J_{sc} \approx 22$ mA cm^{-2}, FF ≈ 0.57, and efficiency $\approx 8.8\%$, respectively. The short circuit current of cell A was higher than cell B and was probably due to the better current collection of cell A for the high band-gap window layer (TO) relative to cell B with the smaller band gap of CdS window layer. Also, though the CdS film was highly transparent, the resulting resistivity could reduce the fill factor and short circuit current as compared to ITO. Figure 2 shows the spectral response of both cells A and B. For cell A, the quantum yield is fairly constant above 500 nm and falls sharply at approximately 800 nm, the CdTe band edge. Below 500 nm, cell A showed a gradual decrease of quantum yield as the SnO_2 cutoff was far away from 500 nm, whereas cell B showed a sharp fall indicating the junction with CdS as the window layer. Though above 500 nm the quantum yield is a little higher for cell B relative to cell A, over all the area under the graph for cell A is higher than that for cell B. The smaller current collection above 500 nm for cell A was probably due to the current loss for the higher lattice mismatch between SnO_2/CdTe of cell A relative to CdS/CdTe of cell B.

Figures 3(a) and 3(b) show the J-V characteristics in the dark of cells A and B, respectively, at different temperatures. Above 300 K, the current density of both cell A and cell B follow the relations:

$$J = J_0 \exp[-(q/AkT)V], \tag{1}$$

$$J = J_0 \exp(-\alpha V), \tag{2}$$

where J_0 is the reverse saturation current, A is the diode quality factor, k is the Boltzmann's constant, T is the temperature, and α is the voltage factor. At lower temperatures, below 230 K, a departure from exponential variation increases with decreasing temperatures indicating complex current mechanisms at lower temperatures. The reverse saturation current can be written as

$$J_0 = J_{00} \exp(-E_a/KT), \tag{3}$$

where E_a is the activation energy and J_{00} is a weak function of temperature.

Figure 4 shows the $\log J_0$ vs $1/T$ for cells A and B of Fig. 1. The slopes gave the activation energies as 0.60 and

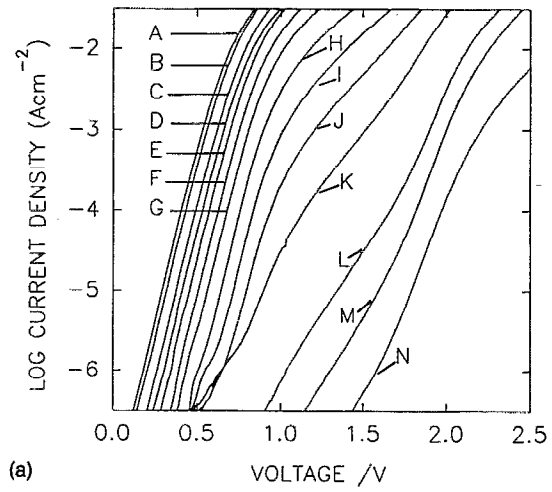

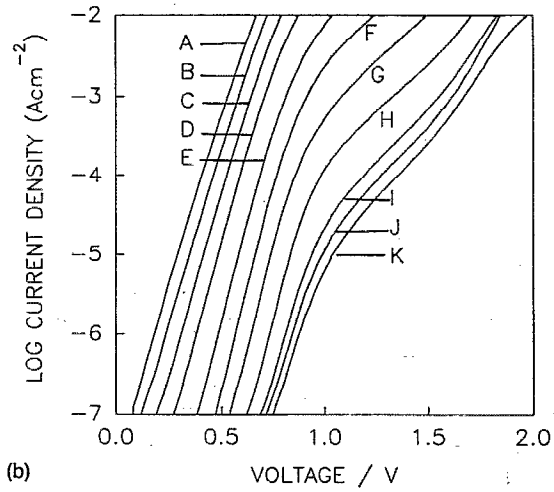

FIG. 3. Current density vs voltage (J-V) characteristic in dark for (a) cell A: *A*:326 K, *B*: 318 K, *C*: 307 K, *D*: 293 K, *E*: 284 K, *F*: 273 K, *G*: 261 K, *H*: 246 K, *I*: 233 K, *J*: 223 K, *K*: 216 K, *L*: 203 K, *M*: 173 K, and *N*: 155 K. (b) cell B: *A*: 323 K, *B*: 315 K, *C*: 307 K, *D*: 296 K, *E*: 281 K, *F*: 273 K, *G*: 252 K, *H*: 238 K, *I*: 209 K, *J*: 196 K, and *K*: 179 K.

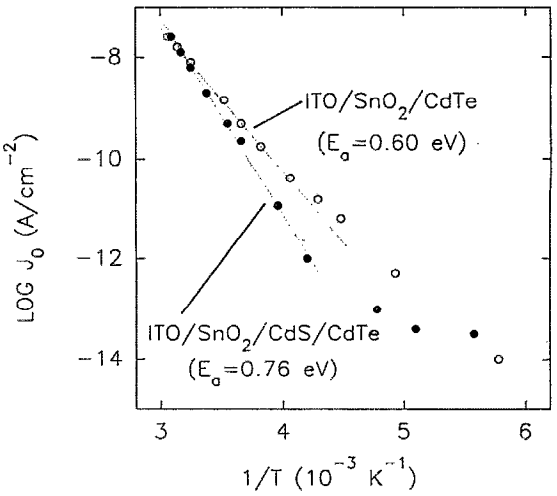

FIG. 4. Temperature dependence of saturation current of cells A and B of Fig. 1.

0.76 eV, respectively, for cells A and B. Anthony *et al.*[1] got 0.67 eV as the activation energy for their CdS/CdTe junction where CdTe has been deposited by C.S.V.T. Werthen *et al.*[17] got 0.76 eV as the activation energy for their ITO/CdTe cell where CdTe has been deposited by evaporation. The product AE_a at room temperature for cells A and B was 1.17 and 1.4 eV, respectively. The product AE_a for cell A was very close to the built-in potential 1.1 eV as measured by a Mott–Schottky plot, whereas the product AE_a for cell B was much higher than the built-in potential of 0.95 eV. Figure 5 shows the temperature dependence of the diode quality factor A and the voltage factor α for both cells A and B. The values of the ideality factor A for cell B lying between 1.8 at 323 K and 2.06 at 227 K and suggest that the recombination may be the dominant junction transport mechanism in cell B. Again, the variation of the voltage factor α with temperature indicates that the thermally assisted tunneling could be an alternative mechanism of junction transport in cell B. For cell A the value of A is sensitive to temperature, whereas the voltage factor α is almost temperature independent. These data indicate that tunneling could be an important junction transport mechanism in cell A. Figure 6 shows the temperature dependence of open circuit voltage of cells A and B. Built-in potentials of both cells were found by extrapolating the graphs to $T=0$ K and found to be 1.41 and 1.5 eV for cells A and B, respectively. These values of built-in potential were higher than those measured by capacitance measurements.

Figure 7 shows the frequency dispersion of capacitance of cells A and B of Fig. 1. Cell B had a higher frequency dispersion than cell A. The cell associated with a wide range of energy levels and time constants shows a higher value of capacitance at lower frequencies where more deep levels can respond to the ac signal. The total number of states due to depletion and interface can be measured from the measured capacitance at lower frequency ($\approx$10 Hz),

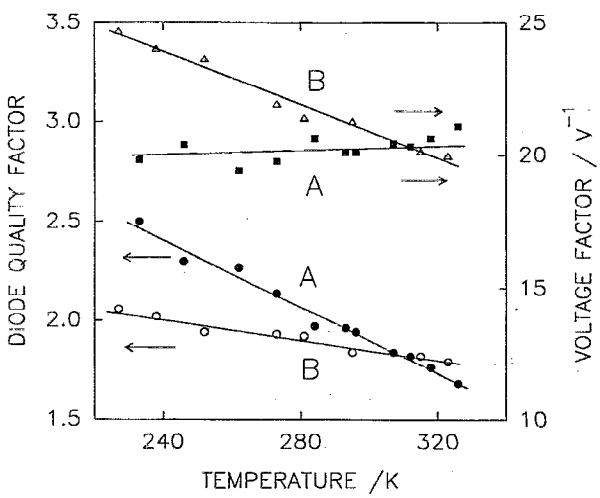

FIG. 5. Temperature dependence of diode quality factor and voltage factor of cells A and B of Fig. 1.

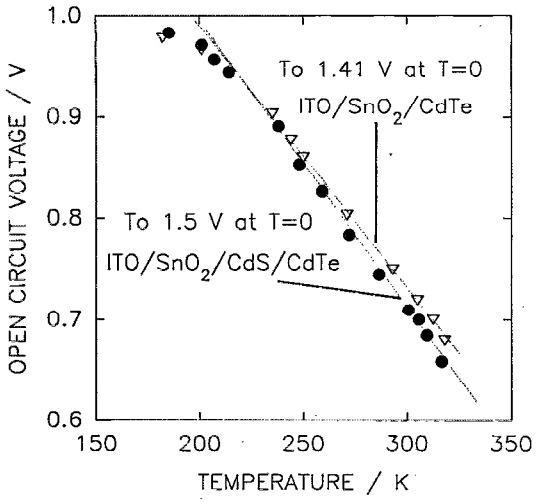

FIG. 6. Temperature dependence of open circuit voltage of cells A and B of Fig. 1.

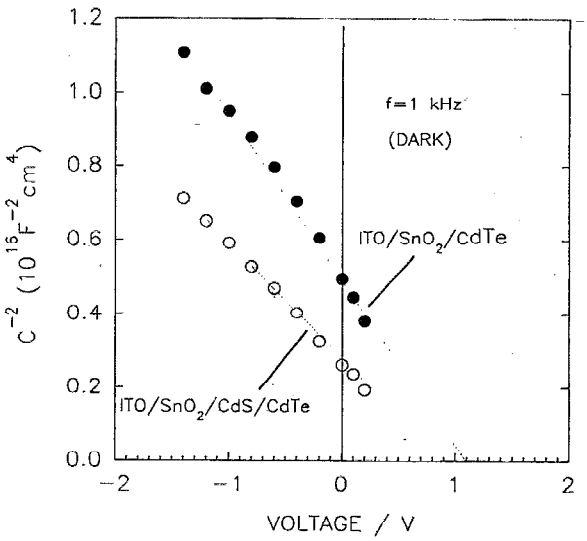

FIG. 8. Mott–Schottky plot of cells A and B of Fig. 1.

whereas the capacitance at higher frequency ($\approx 10^5$ Hz) is associated with depletion only. The number of interface states can be calculated from the measured capacitances at low and high frequencies by using the relation[25]

$$N_{IS}=(C_{LF}-C_{HF})/q, \tag{4}$$

where N_{IS} is the total number of interface states, C_{LF} and C_{HF} are the measured capacitances at lower (≈ 10 Hz) and higher ($\approx 10^5$ Hz) frequencies, respectively, and q is the electronic charge. The number of interface states for cells A and B at dark and zero volt bias were 1.7×10^{11} and 3.0×10^{11} eV^{-1} cm^{-2}, respectively.

Figure 8 shows the Mott–Schottky plots of both cells A and B of Fig. 1 at 10 kHz frequency. The slopes of the graphs gave the values of carrier concentrations and were 1.9×10^{15} and 4.5×10^{15} cm^{-3} for cells A and B, respectively. The voltage intercepts at $C^{-2}=0$ gave the values of built-in potential, V_{bi} and were 1.1 and 0.95 eV for cells A and B, respectively. Mitchell *et al.*[19] got 1.4 eV as V_{bi} for their glass/SnO_2/CdTe solar cell from a C^{-2} versus voltage plot.

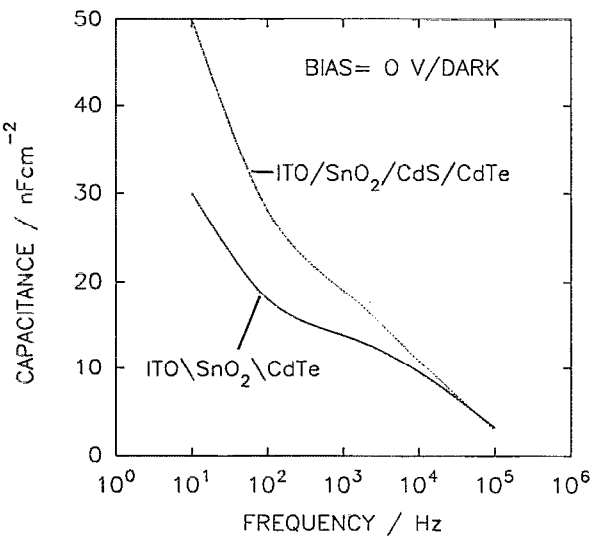

FIG. 7. Frequency dispersion of capacitance of cells A and B of Fig. 1.

IV. CONCLUSION

CdTe has been electrodeposited to fabricate two types of solar cells as ITO/SnO_2/CdTe and ITO/SnO_2/CdS/CdTe structures. Due to the high band gap of SnO_2 relative to CdS, the current collection of the ITO/SnO_2/CdTe cell was higher than that of the ITO/SnO_2/CdS/CdTe cell and was observed from spectral response measurements. The high current collection gave a higher short circuit current (J_{sc}) for the ITO/SnO_2/CdTe cell relative to the ITO/SnO_2/CdS/CdTe cell. Current-voltage temperature measurements suggest that the junction transport could be controlled by recombination or thermally assisted tunneling in the ITO/SnO_2/CdTe cell, whereas tunneling could be the important junction transport mechanism in the ITO/SnO_2/CdS/CdTe cell. The capacitance measurements showed that the frequency dispersion was higher for the ITO/SnO_2/CdS/CdTe cell relative to the ITO/SnO_2/CdTe cell. The interface states were measured from lower (≈ 10 Hz) and higher ($\approx 10^5$ Hz) frequencies measurements and were found to be 1.7×10^{11} and 3×10^{11} cm^{-2} eV^{-1}, respectively. Mott–Schottky plots gave the value of built-in potential of ITO/SnO_2/CdTe and ITO/SnO_2/CdS/CdTe cells as 1.1 and 0.95 V, respectively, whereas the temperature dependence of open circuit voltage gave the built-in potential as 1.41 and 1.5 V, respectively, for those cells. Depositing a CdS layer in between transparent conducting oxide (TCO) and CdTe did not improve the overall performance of the solar cell. More research on TCO/CdTe is necessary to get a high efficiency with high V_{oc} and high J_{sc} and can easily eliminate CdS layer to reduce the cost.

ACKNOWLEDGMENTS

Philip Tanner is thanked for valuable discussions. The research was supported by the Energy Research Development Corporation and Australian Research Committee.

[1] T. C. Anthony, A. L. Fahrenbruch, M. G. Peters, and R. H. Bube, J. Appl. Phys. **57**, 400 (1985).
[2] Y. Tyan and E. A. Perez-Albuerre, *Proceedings of the 16th IEEE Photovoltaic Specialists' Conference*, San Diego, California (IEEE, New York, 1982), p. 794.
[3] K. W. Mitchell, C. Eberspacher, F. Cohen, J. Avery, G. Duran, and W. Bottenberg, *Proceedings of the 18th Photovoltaic Specialists' Conference*, Las Vegas, Nevada (IEEE, New York, 1985), p. 1359.
[4] T. L. Chu, S. S. Chu, S. T. Ang, K. D. Han, Y. Z. Liu, K. Zweibel, and H. S. Ullal, *Proceedings of the 19th Photovoltaic Specialists' Conference*, New Orleans, Louisiana (IEEE, New York, 1987), p. 1466.
[5] H. Matsumoto, K. Kuribayashi, H. Uda, Y. Komatsu, N. Nakano, and S. Ikegami, Sol. Cells **11**, 367 (1984).
[6] S. Ikegami, Sol. Cells **23**, 89 (1988).
[7] B. M. Basol, Sol. Cells **23**, 69 (1988).
[8] P. V. Meyers, Sol. Cells **23**, 59 (1988).
[9] B. M. Basol, J. Appl. Phys. **55**, 601 (1984).
[10] G. C. Morris, A. Tottszer, and S. K. Das, Mater. Forum **15**, 164 (1991).
[11] C. G. Morris, S. K. Das, and P. G. Tanner, J. Cryst. Growth **117**, 429 (1992).
[12] C. G. Morris and S. K. Das, Int. J. Sol. Energy (in press).
[13] J. M. Woodcock, A. K. Turner, M. E. Ozsan, and J. G. Summer, *Proceedings of the 22nd IEEE Photovoltaic Specialists' Conference*, Las Vegas, Nevada (IEEE, New York, 1991), p. 842.
[14] R. W. Birkmire, B. E. McCandless, and W. N. Sharfarman, Sol. Cells **23**, 115 (1988).
[15] T. Nakazawa, K. Takamizwa, and K. Ito, Appl. Phys. Lett. **50**, 279 (1987).
[16] J. G. Werthen, T. C. Anthony, A. L. Fahrenbruch, and R. H. Bube, *Proceedings of the 16th IEEE Photovoltaic Specialists' Conference*, San Diego, California (IEEE, New York, 1982), p. 1138.
[17] J. G. Werthen, A. L. Fahrenbruch, R. H. Bube, and J. C. Zesch, J. Appl. Phys. **54**, 2750 (1983).
[18] F. G. Courreges, A. L. Fahrenbruch, and R. H. Bube, J. Appl. Phys. **51**, 2175 (1980).
[19] K. W. Mitchell, C. Eberspacher, F. Cohen, J. Avery, G. Duran, and W. Bottenberg, Sol. Cells **23**, 49 (1988).
[20] M. Ginting and J. D. Leslie, Can. J. Phys. **67**, 444 (1989).
[21] M. S. Tomer, Thin Solid Films **164**, 295 (1988).
[22] J. A. Aranovich, D. Golmayo, A. L. Fahrenbruch, and R. H. Bube, J. Appl. Phys. **51**, 4260 (1980).
[23] M. P. R. Panicker, M. Knaster, and F. A. Kroger, J. Electrochem. Soc. **125**, 556 (1978).
[24] B. M. Basol, E. S. Tseng, and R. L. Rod, US Patent No. 4 388 483 (14 June, 1983).
[25] H. Tavakolian and J. R. Sites, *Proceedings of the 20th Photovaltaic Specialists' Conference*, Las Vegas, Nevada (IEEE, New York, 1988), p. 1608.